ÉCOLE POLYTECHNIQUE
FÉDÉRALE DE LAUSANNE

Semester Project Report:

Hydropter
Modeling & Control

Student: **Amine Merdassi**

Professor: **Dominique Bonvin**

Assistants: **Philippe Mullhaupt and Sébastien Gros**

Table of Contents

1. Introduction:

The Hydropter is a sailing boat using hydrofoils (lifting surfaces operating in liquids). The hydrofoils generate enough lift to carry the boat and balance the forces produced by the sails at a level of drag far inferior to those obtained with classical hulls: the boat flies on the water. The speeds reached by the hydropter exceed largely those obtained with standard sailing boats. The main drawback of this type of system is the lack of stability with respect to waves and the difficult steering.

This paper presents the procedure of hydropter modeling and describes different approaches to control the system. The structure has 4 inputs and 12 states. It is a fast and strongly nonlinear system. The control schemes are computed based on a simplified model of the system. The hydropter model is derived using Lagrange-Euler Approach.

The first control approach is based on optimal control scheme. Linear Quadratic Regulator (LQR) theory is used to design a state feedback controller. The goal is to use LQR theory to suppress flutter and to maintain stability of the closed loop system. The second control approach consists of a standard way to control nonlinear systems. The idea is to use optimization-based Model Predictive Control (MPC). Therein, the problem of control is formulated as an optimization problem. The goal is to generate reference input and state trajectories in order to change dynamically the setpoints.

The paper is organized as follows. Section 2 describes the steps followed to model the hydropter. System linearization is briefly reviewed in Section 3. The LQR control approach is then presented in section 4 and some results are commented. The Model Predictive Control (MPC) is detailed in Section 5 with some implementation results. Finally, conclusions are provided in Section 6.

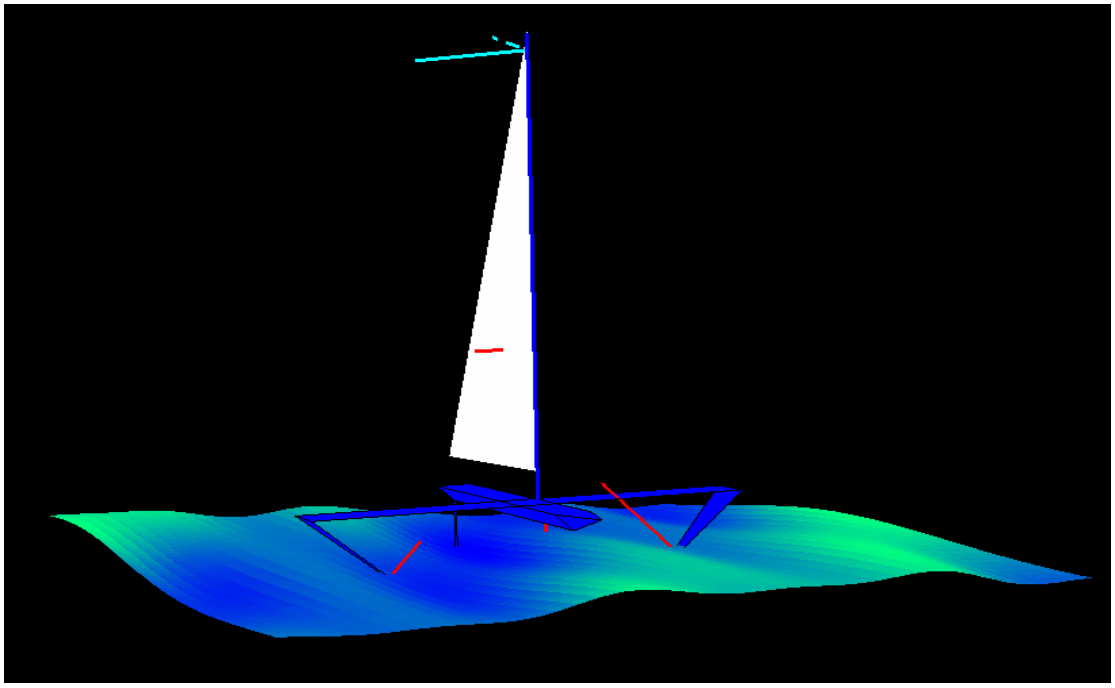

2. Hydropter Modeling:

2.1 Aerodynamic Forces for a hydrofoil:

The figure below shows the section of the hydrofoil. The chord is the line between the leading and the trailing edge and the angle between the relative speed and this chord is the angle of attack (Aoa). As every other solid moving in a fluid *[1]* at a certain speed, one can represent the sum of all aerodynamic forces acting on the wing with two perpendicular forces: the lift force F_l and the drag force F_d that are respectively perpendicular and parallel to the speed vector.

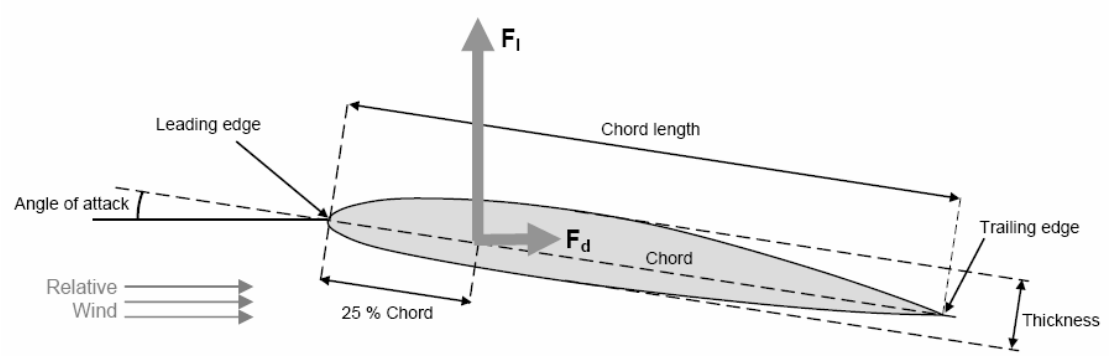

Figure 1: *Section of the hydrofoil and the lift and drag forces*

$$F_l = C_l \frac{\rho}{2} S v^2$$

$$F_d = C_d \frac{\rho}{2} S v^2$$

$$M = C_m \frac{\rho}{2} S v^2 \cdot chord$$

with
- ρ : Density of fluid (air)
- S : Wing area
- v : Flight speed (relative to surrounding fluid)
- C_L : Lift coefficient
- C_D : Drag coefficient
- C_M : Moment coefficient

The lift, drag and moment coefficients depend on the hydrofoil, the angle of attack and a third value that is the Reynolds number. It is representative of the viscosity of the fluid but will not be explained more in details.

2.2 Orientation of the Hydropter:

Let's consider:

Earth fixed frame: $E = \{E_X, E_Y, E_Z\}$

Body fixed frame: $B = \{E_x, E_y, E_z\}$

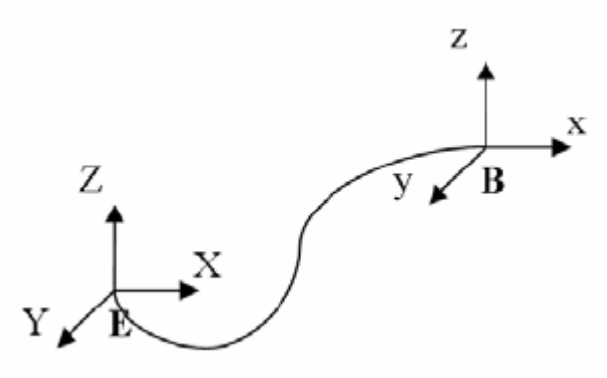

Figure 2: *General Coordinate System*

At each moment, we need to know the position and the orientation of B relative to E.

The transformation consists of three successive rotations:

- *Rotation of ϕ around $\vec{x}$* **Roll** ($-\pi/2<\phi<\pi/2$)
- *Rotation of θ around $\vec{y}$* **Pitch** ($-\pi/2<\theta<\pi/2$)
- *Rotation of ψ around $\vec{z}$* **Yaw** ($-\pi<\psi<\pi$)

The complete rotation matrix, called *Direct Cosine Matrix* is then

$$R(\phi,\theta,\psi) = R(z,\psi)\cdot R(y,\theta)\cdot R(x,\phi)$$

$$R(\phi,\theta,\psi) = \begin{bmatrix} \cos\psi & -\sin\psi & 0 \\ \sin\psi & \cos\psi & 0 \\ 0 & 0 & 1 \end{bmatrix} \cdot \begin{bmatrix} \cos\theta & 0 & \sin\theta \\ 0 & 1 & 0 \\ -\sin\theta & 0 & \cos\theta \end{bmatrix} \cdot \begin{bmatrix} 1 & 0 & 0 \\ 0 & \cos\phi & -\sin\phi \\ 0 & \sin\phi & \cos\phi \end{bmatrix}$$

$$R(\phi,\theta,\psi) = \begin{bmatrix} \cos\psi\cos\theta & \cos\psi\sin\theta\sin\phi - \sin\psi\cos\phi & \cos\psi\sin\theta\cos\phi + \sin\psi\sin\phi \\ \sin\psi\cos\theta & \sin\psi\sin\theta\sin\phi + \cos\psi\cos\phi & \sin\psi\sin\theta\cos\phi - \sin\phi\cos\psi \\ -\sin\theta & \cos\theta\sin\phi & \cos\theta\cos\phi \end{bmatrix}$$

2.3 Model derivation using Lagrange-Euler Approach:

The Lagrange-Euler approach is based on the concept of kinetic and potential energy:

$$\Gamma_i = \frac{d}{dt}\left(\frac{\delta L}{\delta \dot{q}_i}\right) - \frac{\delta L}{\delta q_i}$$
$$L = T - V$$

avec q_i : generalized coordinates
Γ_i : generalized forces given by non-conservatives forces
T : total kinetic energy
V : total potential energy

The kinetic energy due to the translation is immediately:

$$E_{cin\,translation} = \frac{1}{2}m\dot{x}^2 + \frac{1}{2}m\dot{y}^2 + \frac{1}{2}m\dot{z}^2$$

Assuming that the inertia matrix is diagonal, the kinetic energy due to the rotation is:

$$E_{cin\,rotation} = \frac{1}{2}I_{xx}\omega_x^2 + \frac{1}{2}I_{yy}\omega_y^2 + \frac{1}{2}I_{zz}\omega_z^2$$

Where $\omega_x, \omega_y, \omega_z$ are the rotational speed that can be expressed as a function of the roll, pitch and yaw rate $(\dot{\phi}, \dot{\theta}, \dot{\psi})$:

$$\begin{pmatrix} \omega_x \\ \omega_y \\ \omega_z \end{pmatrix} = \begin{pmatrix} \dot{\phi} - \dot{\psi}\cdot\sin\theta \\ \dot{\theta}\cdot\cos\phi + \dot{\psi}\cdot\sin\phi\cos\theta \\ -\dot{\theta}\cdot\sin\phi + \dot{\psi}\cdot\cos\phi\cos\theta \end{pmatrix}$$

This leads to the total kinetic energy:

$$T = \frac{1}{2}\left(m\dot{x}^2 + m\dot{y}^2 + m\dot{z}^2 + I_{xx}\omega_x^2 + I_{yy}\omega_y^2 + I_{zz}\omega_z^2\right)$$

The potential energy can be expressed by:

$$V = -m\cdot g\cdot Z = -m\cdot g\cdot\left(-\sin\theta\cdot x + \sin\phi\cos\theta\cdot y + \cos\phi\cos\theta\cdot z\right)$$

The Lagrangian is :

$$L = T - V$$

The motion equations are then given by:

$$\frac{d}{dt}\left(\frac{\partial L}{\partial \dot{x}}\right) - \frac{\partial L}{\partial x} = F_x \qquad \frac{d}{dt}\left(\frac{\partial L}{\partial \dot{y}}\right) - \frac{\partial L}{\partial y} = F_y \qquad \frac{d}{dt}\left(\frac{\partial L}{\partial \dot{z}}\right) - \frac{\partial L}{\partial z} = F_z$$

$$\frac{d}{dt}\left(\frac{\partial L}{\partial \dot{\psi}}\right) - \frac{\partial L}{\partial \psi} = \tau_\psi \qquad \frac{d}{dt}\left(\frac{\partial L}{\partial \dot{\phi}}\right) - \frac{\partial L}{\partial \phi} = \tau_\phi \qquad \frac{d}{dt}\left(\frac{\partial L}{\partial \dot{\theta}}\right) - \frac{\partial L}{\partial \theta} = \tau_\theta$$

After calculation, we obtain the left parts of equations above:

$$\frac{d}{dt}\left(\frac{\partial L}{\partial \dot{x}}\right)-\frac{\partial L}{\partial x}=m\ddot{x}+mg\sin\theta$$

$$\frac{d}{dt}\left(\frac{\partial L}{\partial \dot{y}}\right)-\frac{\partial L}{\partial y}=m\ddot{y}-mg\sin\phi\cos\theta$$

$$\frac{d}{dt}\left(\frac{\partial L}{\partial \dot{z}}\right)-\frac{\partial L}{\partial z}=m\ddot{z}-mg\cos\phi\cos\theta$$

$$\frac{d}{dt}\left(\frac{\partial L}{\partial \dot{\phi}}\right)-\frac{\partial L}{\partial \phi}=I_{xx}\dot{\omega}_x-(I_{yy}-I_{zz})\omega_y\omega_z$$

$$\frac{d}{dt}\left(\frac{\partial L}{\partial \dot{\theta}}\right)-\frac{\partial L}{\partial \theta}=-\sin\phi(\dot{\omega}_z I_{zz}-\omega_x\omega_y(I_{xx}-I_{yy}))+\cos\phi(\dot{\omega}_y\cdot I_{yy}-\omega_x\omega_z(I_{zz}-I_{xx}))$$

$$\frac{d}{dt}\left(\frac{\partial L}{\partial \dot{\psi}}\right)-\frac{\partial L}{\partial \psi}=-\sin\theta\cdot(\dot{\omega}_x I_{xx}-\omega_y\omega_z(I_{yy}-I_{zz}))+\sin\phi\cos\theta\cdot(\dot{\omega}_y I_{yy}-\omega_x\omega_z(I_{zz}-I_{xx}))+\cos\phi\cos\theta\cdot(\dot{\omega}_z I_{zz}-\omega_x\omega_y(I_{xx}-I_{yy}))$$

The non-conservative forces and moments come from the hydrodynamics.

Finally, isolating the acceleration we obtain:

$$\begin{cases}\ddot{x}=\dfrac{F_{tot,x}}{m}-g\sin\theta\\ \ddot{y}=\dfrac{F_{tot,y}}{m}+g\sin\phi\cos\theta\\ \ddot{z}=\dfrac{F_{tot,z}}{m}+g\cos\phi\cos\theta\\ \ddot{\phi}=\dfrac{I_{yy}-I_{zz}}{I_{xx}}\dot{\psi}\dot{\theta}+\dfrac{M_{tot,x}}{I_{xx}}\\ \ddot{\theta}=\dfrac{I_{zz}-I_{xx}}{I_{yy}}\dot{\psi}\dot{\phi}+\dfrac{M_{tot,y}}{I_{yy}}\\ \ddot{\psi}=\dfrac{I_{xx}-I_{yy}}{I_{zz}}\dot{\theta}\dot{\phi}+\dfrac{M_{tot,z}}{I_{zz}}\end{cases}$$

3. System Linearization:

As we have seen previously, the *Hydropter* model is described by nonlinear differential equations. In this section we will show how to perform local linearization of nonlinear systems in order to process to a linear control. The procedure *[2]* introduced is based on knowledge of nominal system trajectories specified by the states vector and the nominal system inputs.

Consider now the general nonlinear dynamic control system in matrix form:

$$\dot{x} = f(x, u),$$

Where $\mathbf{x}$, $\mathbf{u}$ and $\mathbf{f}$, are respectively, the n-dimensional system state space vector, the r-dimensional input vector, and the n-dimensional vector function. Assume that the nominal (operating) system trajectory is known and that the nominal system input that keeps the system on the nominal trajectory is given.

The partial derivatives represent the Jacobian matrices given by:

$$A = \left.\frac{\partial f}{\partial x}\right|_{x=0,u=0}$$

$$B = \left.\frac{\partial f}{\partial u}\right|_{x=0,u=0}.$$

Note that the Jacobian matrices have to be evaluated at the nominal points described by $\mathbf{x}_0$ and $\mathbf{u}_0$.

With this notation, the linearized system has the form of:

$$\dot{x}(t) = Ax(t) + Bu(t), \quad x(0) = x_0.$$

The states vector is composed by the six degrees of freedom of the system and their velocities. And, the system inputs correspond to the different angles of wedging for the left and right hydrofoils, the pitch and yaw plans of the system. The structure has 4 inputs and 12 states.

4. Linear Control:

In this chapter, the optimal Linear Quadratic Regulator control *[2]* is discussed and applied to the *Hydropter* stabilization problem. In this case, the objective is to find a control function **u**(t) to stabilize the system.

A system is stabilizable if there exists a state feedback control $\mathbf{u} = K_c\mathbf{x}$ such that the closed loop system is exponentially stable. If the system is stabilizable, then the LQR problem has a solution. The idea of feedback control is simple. Take the state, multiply it by a gain matrix denoted by K_c, and add it back to the system. In particular, given the system,

$$\dot{x}(t) = Ax(t) + Bu(t)$$

we want to find the control input

$$u(t) = -K_c x(t)$$

such that the closed loop system

$$\dot{x}(t) = [A - BK_c]x(t)$$

is exponentially stable. This means that there exists an $M > 0$ and a $\gamma > 0$ such that if **x**(t) is the solution to the closed loop system with **x**(0) = **x**0, then

$$\|x(t)\| \leq Me^{-\gamma t}\|x_0\|.$$

One way of finding K_c is by using Linear-Quadratic Regulator (LQR) design. We will state our problem as follows.

Consider the system

$$\dot{x}(t) = Ax(t) + Bu(t), \quad x(0) = x_0.$$

We seek a control $u^\star(t)$ that minimizes the performance measure

$$\min_u J = \int_0^\infty \{\langle Qx(t), x(t)\rangle + \langle Ru(t), u(t)\rangle\}dt$$

It is well known that if an optimal control $u^\star(t)$ exists, it has the form

$$u^\star(t) = -K_c x(t),$$

where K_c is a constant gain matrix. Moreover, the closed loop system

$$\dot{x}(t) = Ax(t) - BK_c x(t) = (A - BK_c)x(t)$$

is stable. The assumption that $R > 0$ ensures that the energy of the control is finite.

Now, we are going to present and give some remarks about the different results that we obtained using LQR control on different cases of simulation.
Actually, we will focus especially on two cases: the *Hydropter* perturbations (based on kind of sea waves) effect, and the hydrofoils wedging angles control effect.

4.1 Open Loop versus LQR Control:

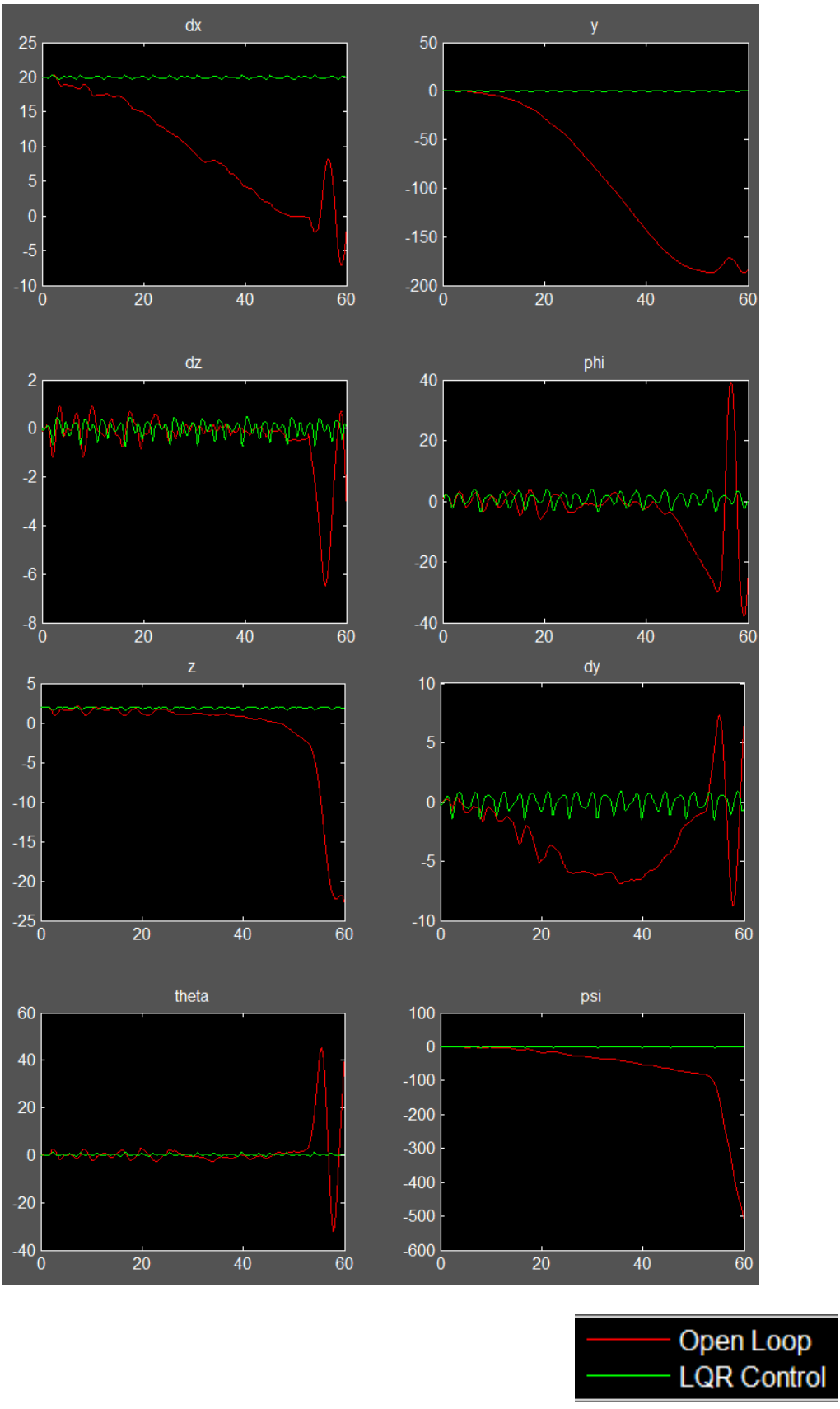

Figure 3 (a): *System states evolution: Open-loop vs LQR Control.*

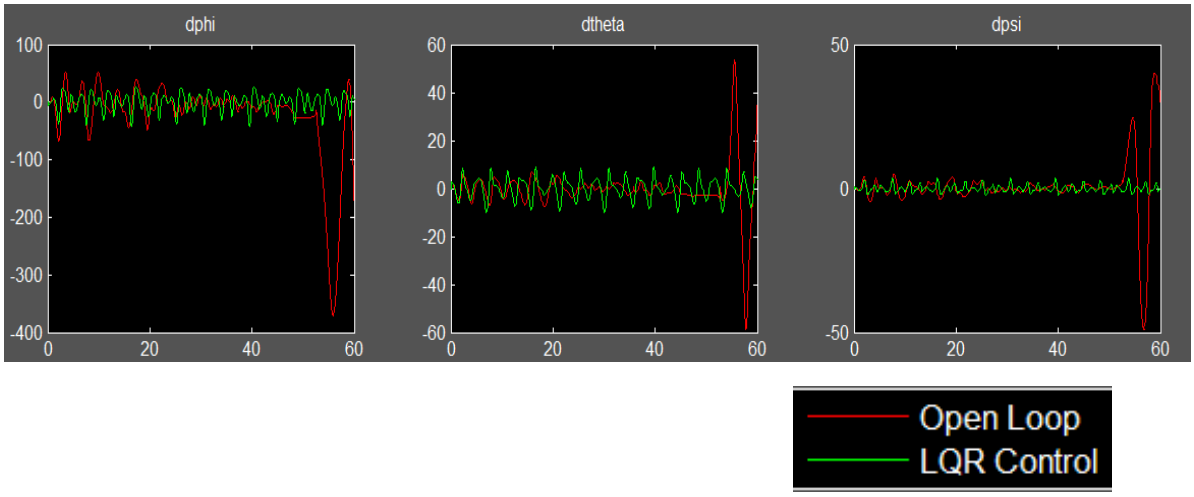

Figure 3 (b): *System states evolution: Open-loop vs LQR Control.*

When we tried to control the system in open-loop, we notice how unstable the system is. The red graphs of the above figures display the behavior of the system states over the time. It's obvious to remark the need of having an optimal control via LQR to make the system stable. The green graphs show the performances of the system controlled by LQR. The system is actually stable with some oscillations due to sea wave perturbations. In the next subsection, we will see how we can influence the magnitude of these oscillations.

4.2 LQR control under sea wave perturbations:

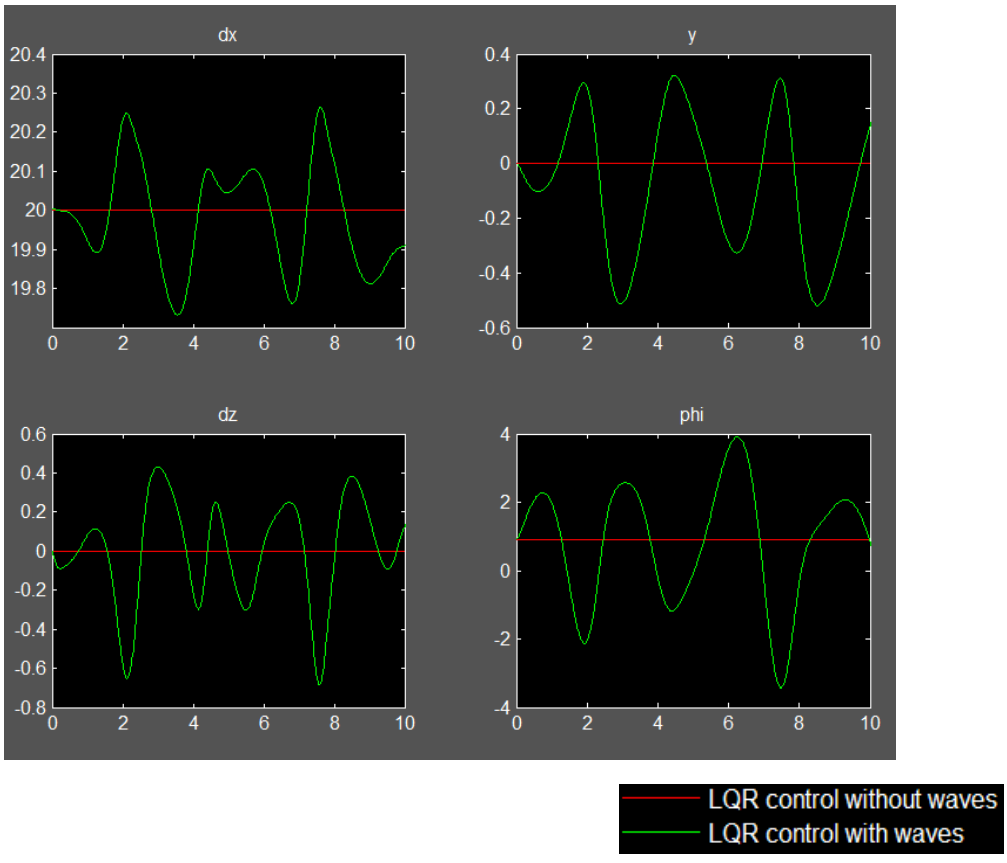

Figure 4 (a): *System states evolution with LQR Control: waves vs no waves.*

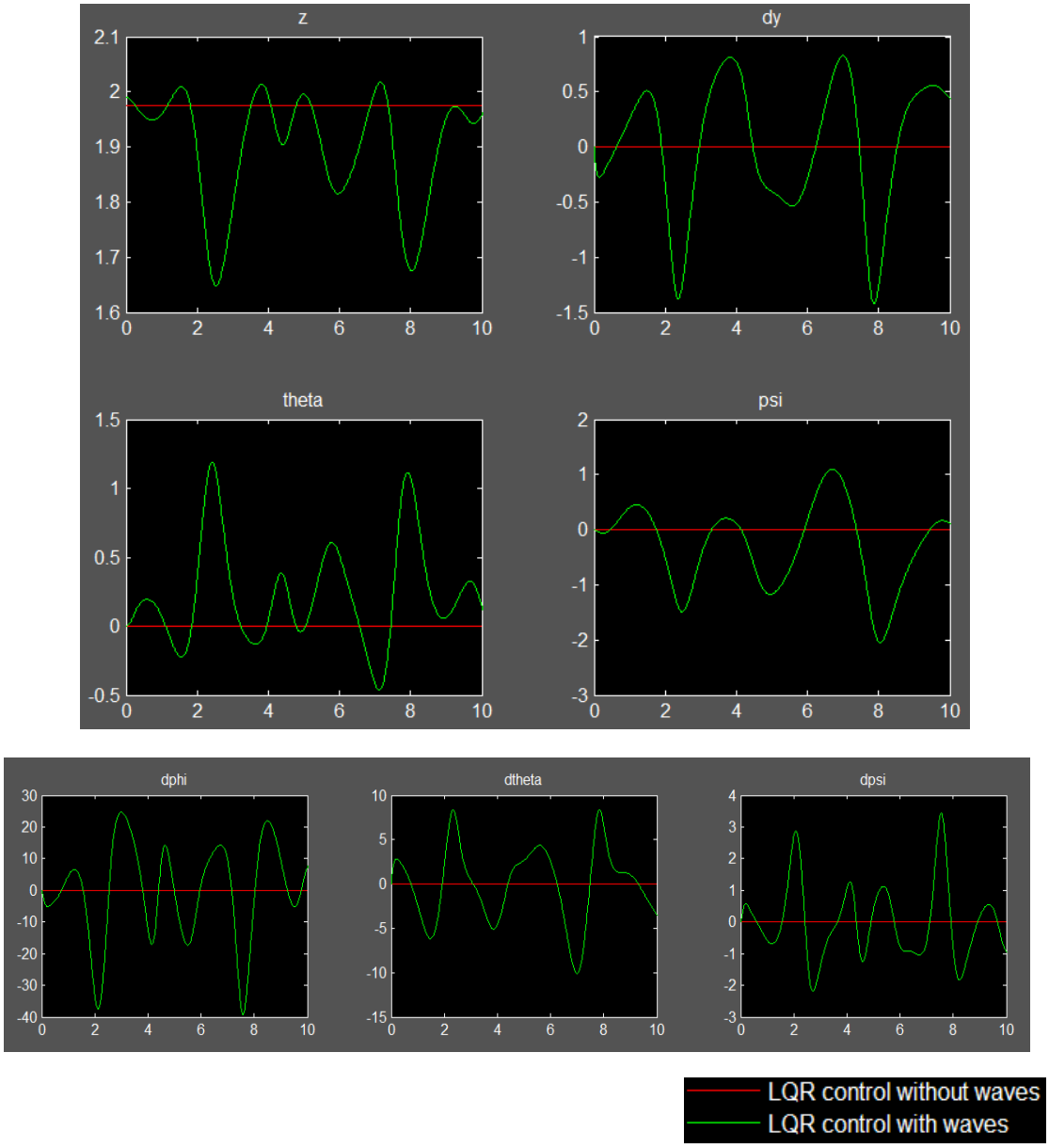

Figure 4 (b): *System states evolution with LQR Control: waves vs no waves.*

The figures above show the evolution over time of the different states of the system under LQR control. The red color is reserved for the no wave perturbations case. In fact, we notice how stable the system is in this ideal case. From the green graphs, which correspond to the LQR control under sea wave perturbations, we remark some oscillations of the different states and despite that the system remains stable over time. Trying different weighting matrices Q and R, we found larger amplitude of oscillations for some states and a smaller for other states.
As a conclusion, we should choose our weighting matrices Q and R considering the oscillations tradeoffs between the system states.

4.3 LQR with hydrofoils control:

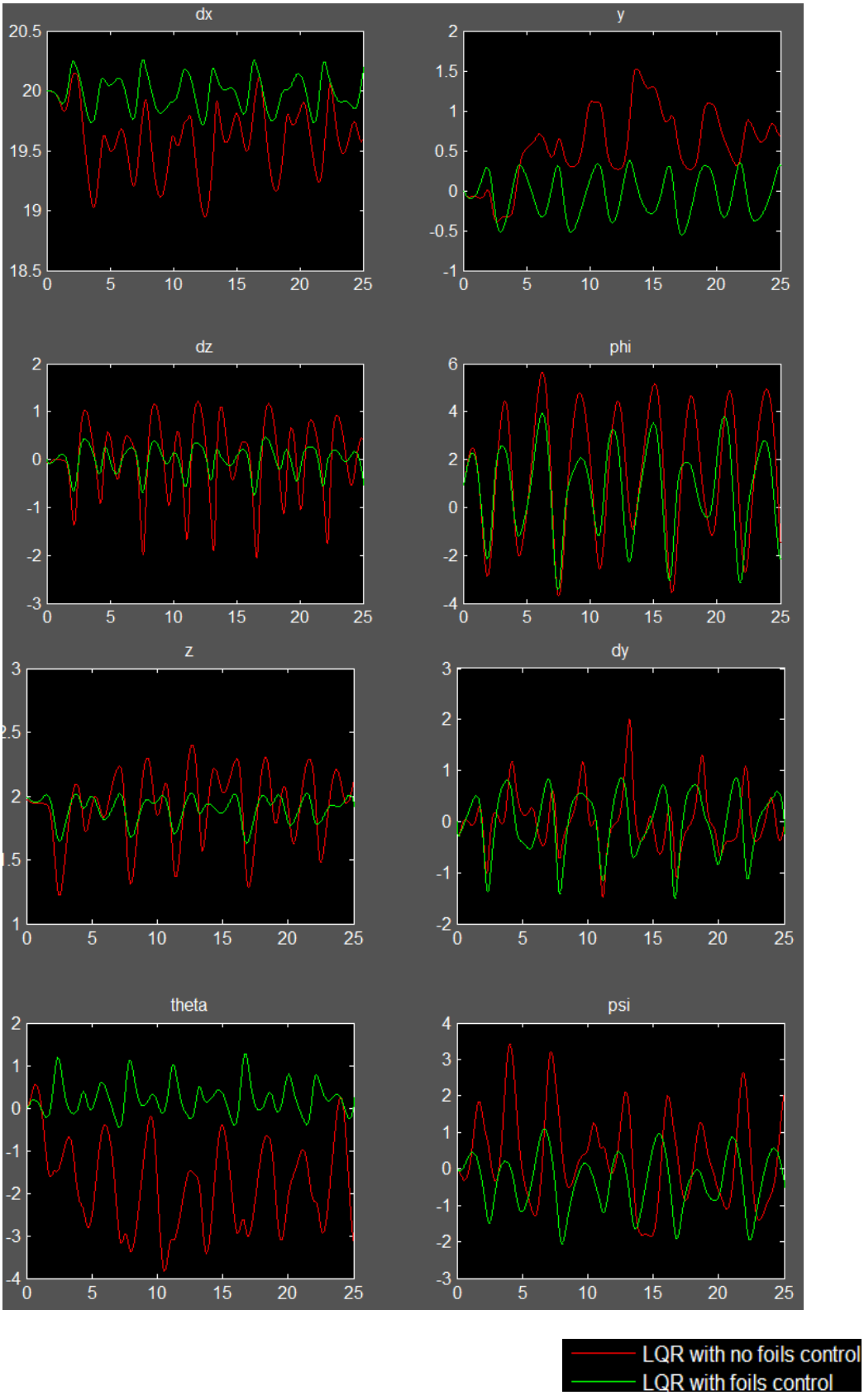

Figure 5 (a): *System states evolution with LQR Control: hydrofoils control vs no hydrofoils control.*

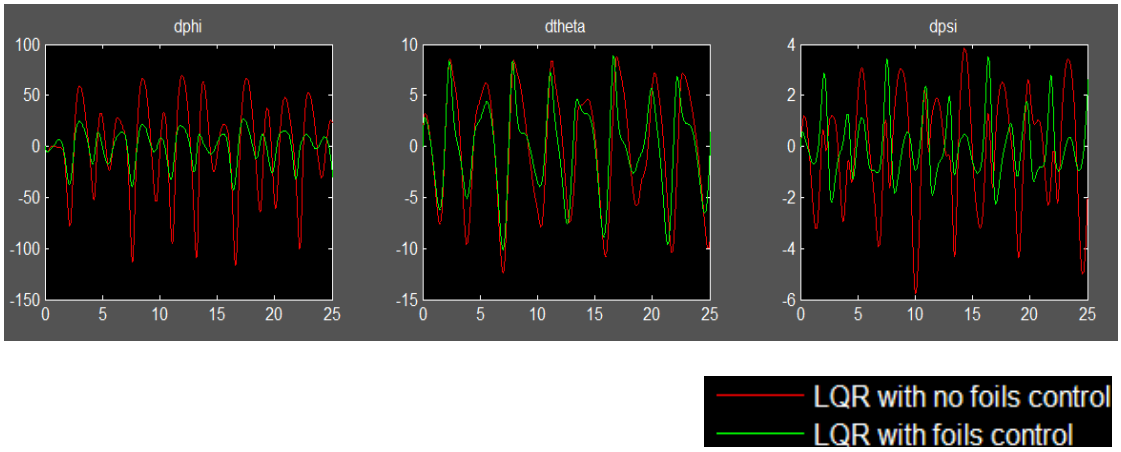

Figure 5 (b): *System states evolution with LQR Control: hydrofoils control vs no hydrofoils control.*

These figures above will help us to explore the hydrofoils wedging angles control effect on the system oscillations with LQR control under sea wave perturbations. The red graphs display the evolution over time of the system states without controlling the hydrofoils wedging angles. Comparing to the performances of the system in green with hydrofoils LQR control, we notice that controlling the hydrofoils seems very important to reduce the sea wave perturbations effect. Actually, despite the fact that the system remains stable for the two cases, applying LQR with hydrofoils control make the system in a better steady state.

5. Nonlinear MPC:

A standard way to control nonlinear systems is to use optimization-based Model Predictive Control (MPC) *[5] [6]*. MPC formulates the problem of input trajectory generation as an optimization problem. The generation of the reference trajectories $u_{ref}(t)$ and $x_{ref}(t)$ can be computed via optimization (e.g. nonlinear MPC) or direct system inversion (as is possible for example for flat systems) *[3] [4]*.

Consider the nonlinear dynamic process:

$$\dot{x} = F(x,u), \qquad x(0) = x_0$$

where the state x and the input u are vectors of dimension n and m, respectively. x_0 represents the initial conditions, and F the process dynamics. The predictive control is based on repeatedly solving the following optimization problem:

$$\begin{aligned} \min_{u[t_k,t_k+T)} \; & J = \Phi(x(t_k+T)) \\ & \quad + \frac{1}{2}\int_{t_k}^{t_k+T} L(x(\tau),u(\tau))d\tau \\ s.t. \quad & \dot{x} = F(x,u), \qquad x(t_k) = x_m(t_k) \\ & \quad \mathcal{S}(x,u) \le 0 \quad \mathcal{T}(x(t+T)) = 0 \end{aligned}$$

where Φ is an arbitrary scalar function of the states and L an arbitrary scalar function of the states and the inputs. $X_m(t)$ represents the measured or estimated value of x(t). $\mathcal{S}$ is a vector function of the states and inputs that represents inequality constraints and $\mathcal{T}$ is a vector function of the final states that represents equality constraints. The horizon of prediction is noted T. The solution to the problem will be noted (x^*, u^*). The size of the re-optimization interval, $\delta = t_{k+1} - t_k$ (sampling time), is lower bounded by the performance of the available optimization tools.

In our case, the choice of cost function for the MPC scheme is:

$$J = \frac{1}{2}\int_{t_k}^{t_k+T} [(\bar{x}-\bar{x}_{sp})^T Q(\bar{x}-\bar{x}_{sp}) + \bar{u}^T R\bar{u}]dt$$

The setpoints correspond to the final states to which the system must be driven. The weighting matrices R and Q are chosen so as to obtain the desired dynamics.
The control problem is of the tracking type: the *Hydropter* structure must be driven smoothly from some initial configuration to another predefined configuration. Actually, we have decided to make the Hydropter accelerating in the x direction from an initial constant speed state. The other speeds and accelerations are zero initially.

In the following subsections, we will treat the results given by trying divers' case of simulations. These results come in the form of reference inputs and states trajectories generated as a solution of the MPC optimization algorithm. In our analysis, we will focus mainly on how to handle some important parameters of the nonlinear MPC optimization problem like prediction horizon T and cost weighting matrices R and Q.

5.1 MPC Horizon effect:

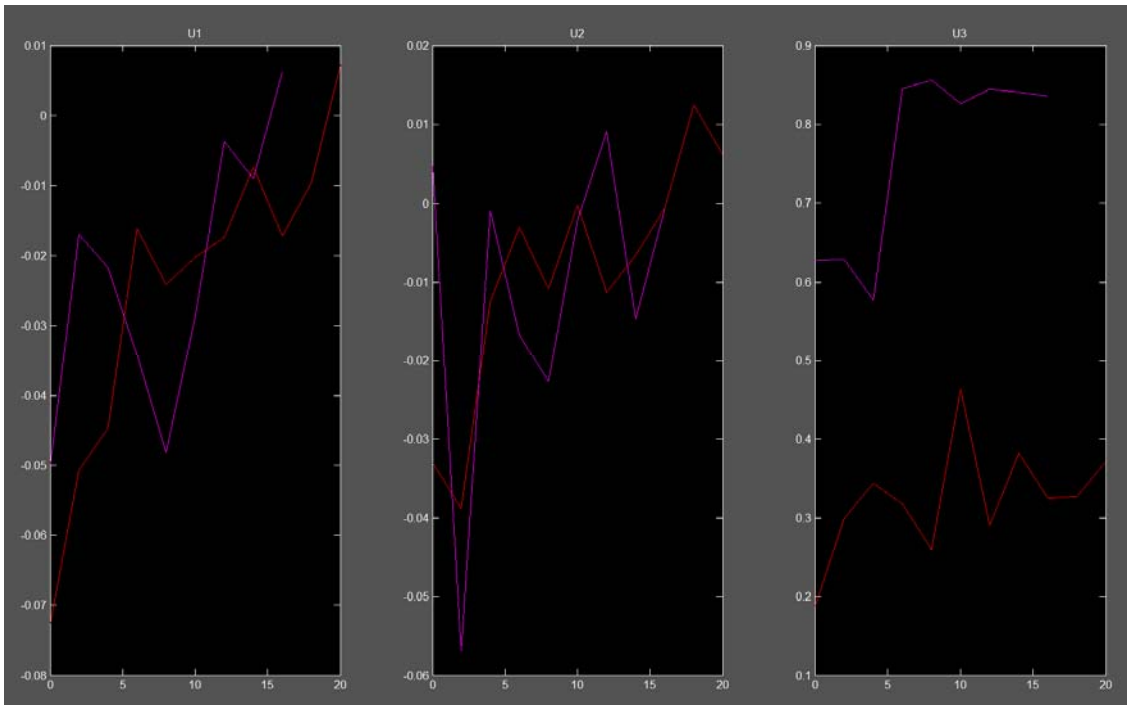

(a)

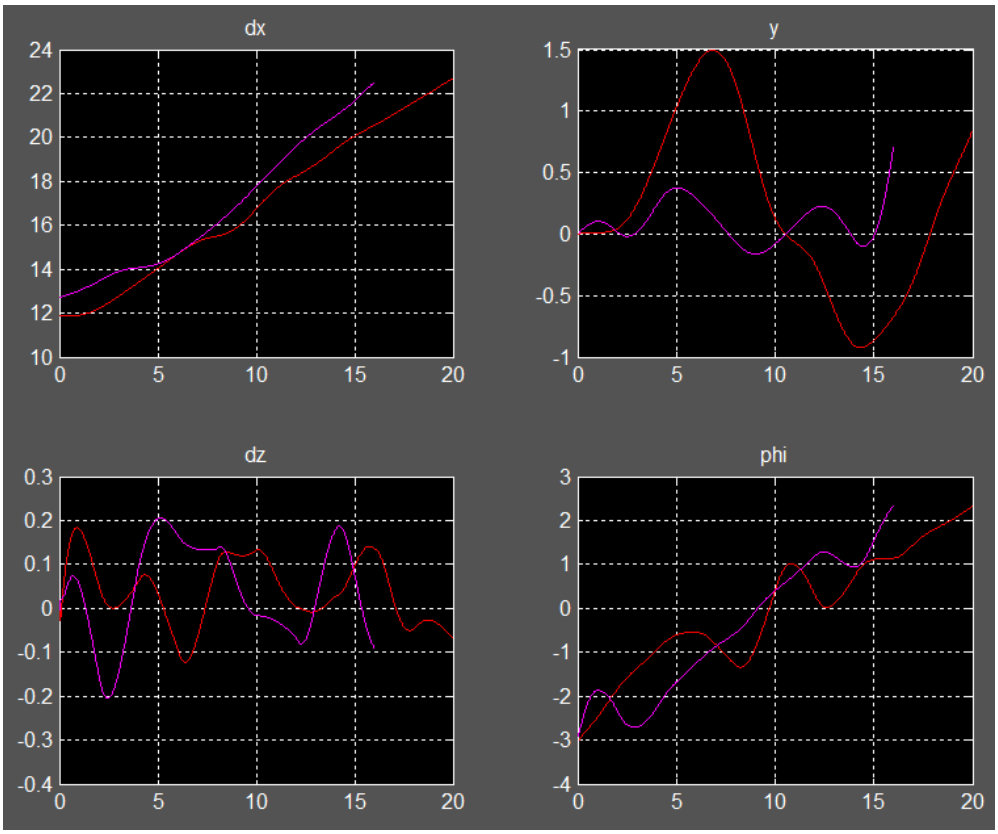

(b)

MPC with Horizon = 20s
MPC with Horizon = 16s

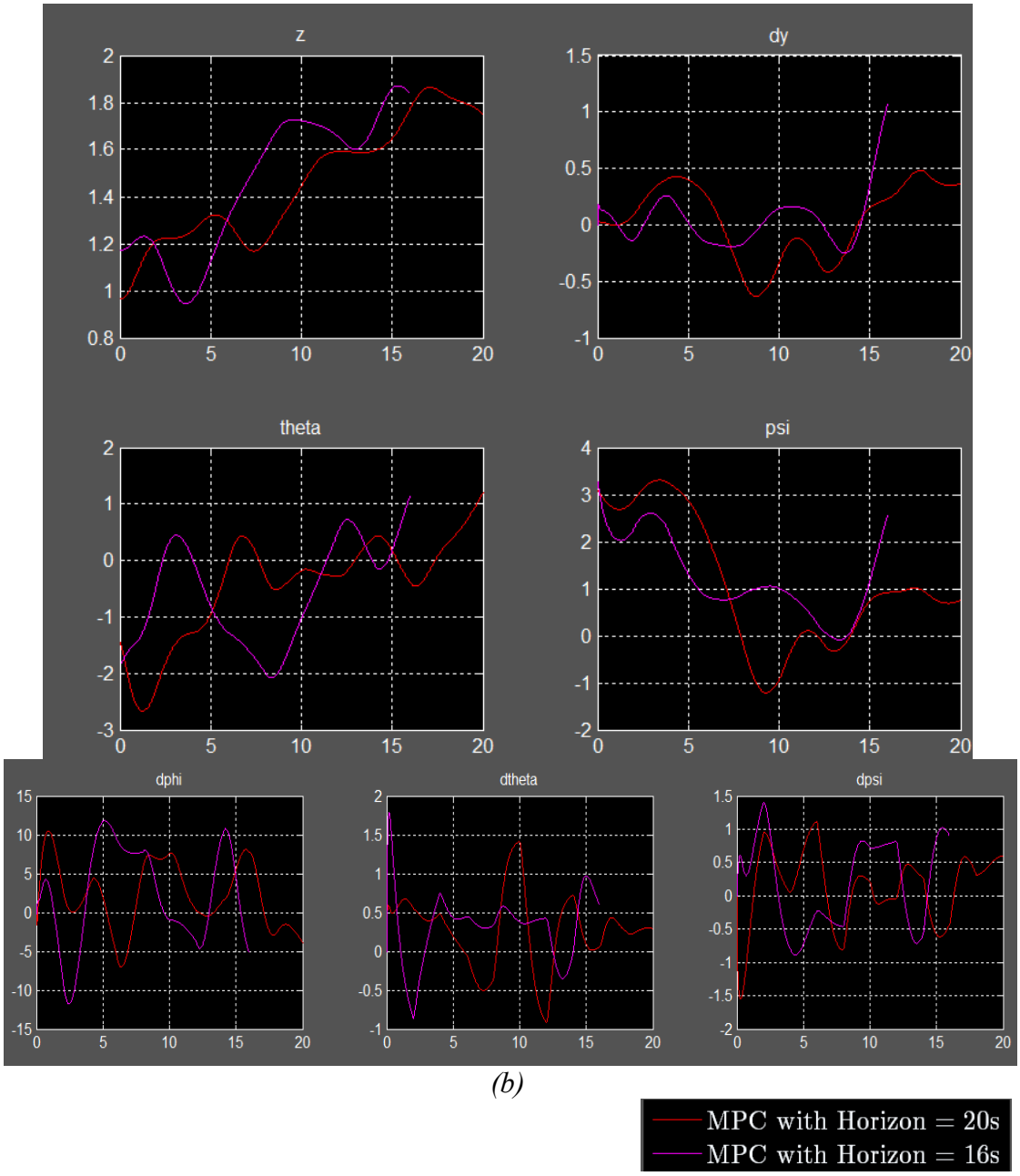

Figure 6: *MPC generated trajectories with different Horizon (20 s & 16 s): (a) Inputs, (b) States.*

The choice of prediction horizon (T) for the nonlinear MPC scheme is not obvious. Too short a prediction horizon tends to lead to stability problems, while too long horizon is not desirable from a computational point of view. The figures above display two kinds of graphs: so, we have the generated reference inputs and states trajectories, in magenta with a prediction horizon of 16 seconds, and in red color with a prediction horizon of 20 seconds. The sampling time $\delta = 2$ [s].
Despite the fact that for a longer horizon, the computational tools take more time to generate the reference trajectories, we notice that through the generated trajectories, the system try to slowly accelerate comparing to a shorter horizon in order to keep the system in a better steady state over the time. As a conclusion the prediction horizon must be chosen according to how fast the available computational tools are.

5.2 MPC weighting matrices effect:

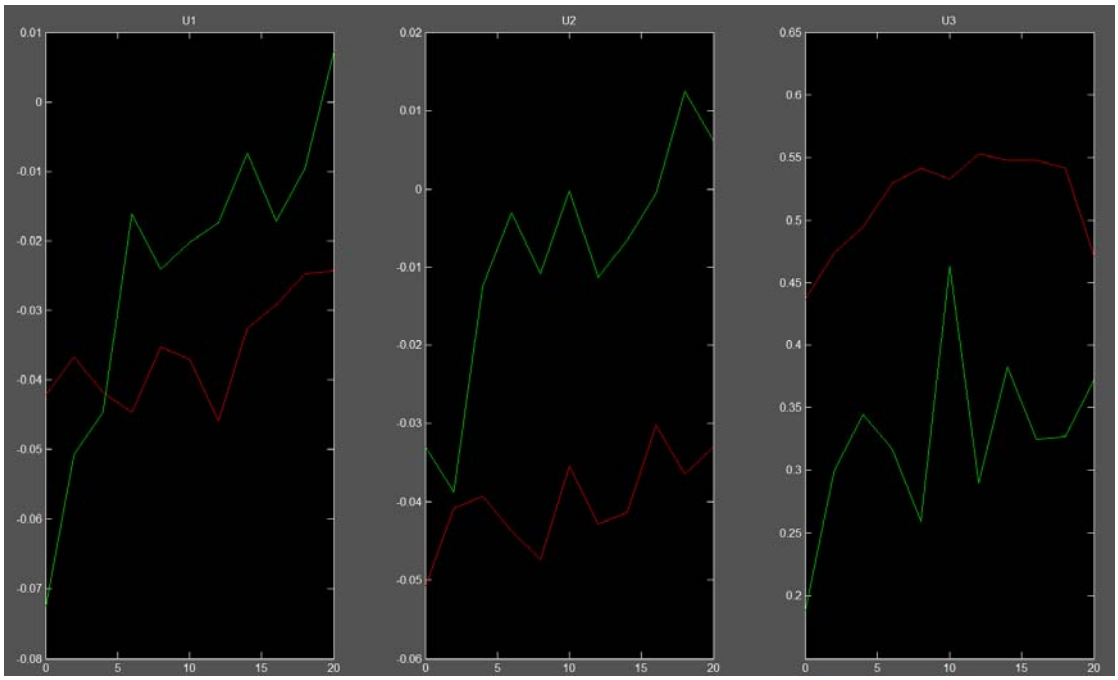

(a)

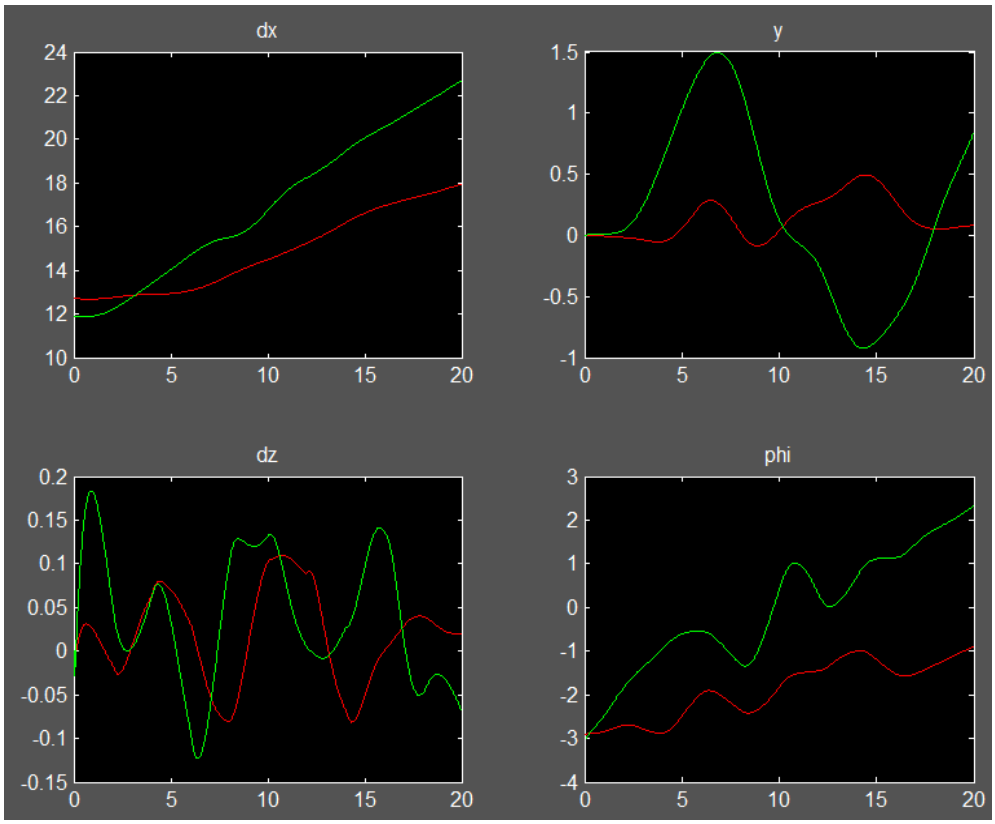

(b)

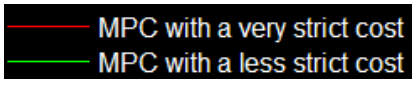

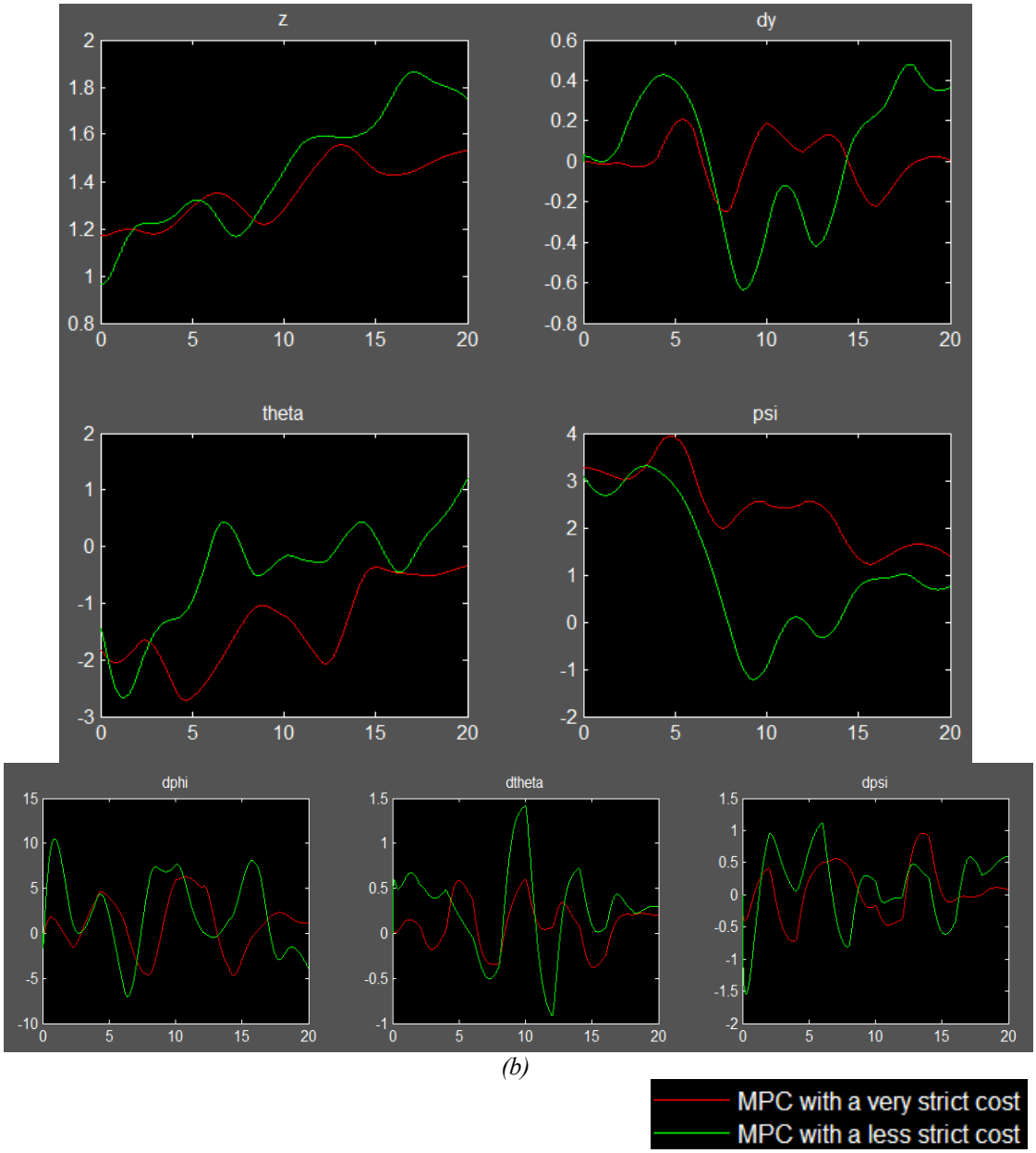

Figure 7: *MPC generated trajectories with different Cost function: (a) Inputs, (b) States.*

The cost function of the nonlinear MPC scheme is characterized by two weighting matrices Q and R. These matrices influence the states oscillations amplitudes over the time. In fact, these oscillations can lead the system to an unstable state. The figures above display two different reference trajectories generated by the nonlinear MPC. The red graphs show that through the weighting matrices Q and R we can improve the dynamic behavior of some states by reducing their oscillation amplitudes comparing to those in green color. Moreover, the red generated reference trajectories perform in a smoother and more stable way. But for this, the price to pay is the system's acceleration. It seems that the system becomes slower despite the fact that we have the same prediction horizon. Hence, we conclude that a tradeoff must be done through these weighting matrices Q and R between the stability of the system over the time and the acceleration wanted.

6. Conclusion:

This paper treated the Hydropter sailing boat in terms of modeling and control approaches. The modeling was described using Lagrange equations. The Control part presented an LQR control for stabilization problem and a nonlinear MPC scheme for reference trajectories generation to a setpoint change.
The MPC methodology is widely used in the process industry where system dynamics are sufficiently slow to permit its implementation. In contrast, applications of predictive control to fast dynamical systems are rather limited: First, the computational burden of the nonlinear optimization limits the frequency of re-optimization, and second, when the re-optimization interval is large relative to the system dynamics, the predictions are quite sensitive to modeling errors and disturbances.
For small deviations from the optimal solution, a linear approximation of the system and a quadratic approximation of the cost are quite reasonable. In such a case, the theory of neighboring extremals (NE) provides a closed-form solution to the optimization. Thus, as a future step it would be interesting to implement a cascade control combination of predictive control and linear time-varying state feedback based on NE for the control of such a fast nonlinear system.

Amine Merdassi
June 15, 2006

7. References:

[1] *C. Gruber and W. Benoit. "Mécanique Générale" Book. Presses Polytechniques & Universitaires romandes*.

[2] *D. Gillet. "Sytèmes Multivariables" Book. Polycopié du cours de Systèmes Multi-variables* .

[3] *Fliess, M., J. Lévine, Ph. Martin and P. Rouchon (1999). A Lie-Bäcklund approach to equivalence and flatness of nonlinear systems IEEE Trans. Automat. Contr. 38, 700–716*.

[4] *J. Lévine, J. Lottin and J-C. Ponsart (1996). A nonlinear approach to the control of magnetic bearings IEEE Trans. Automat.*

[5] *S. Gros, D. Buccieri, P. Mullhaupt and D. Bonvin. A two-time-scale Control Scheme for Fast Unconstrained Systems. Internal Report. Laboratoire d'Automatique, Ecole Polytechnique Fédérale de Lausanne*.

[6] *S. Gros, B. Srinivasan and D. Bonvin. Experimental Illustration of Model Predictive Control for Fast Systems. Internal Report. Laboratoire d'Automatique, Ecole Polytechnique Fédérale de Lausanne*.

8. Appendix:

Matlab .m Files.